

A VLF TRANSMITTER ON THE SPACE SHUTTLE

U. S. Inan, T. F. Bell, R. A. Helliwell and
K. P. Katsufakis

*Radioscience Laboratory, Stanford University, Stanford,
California 94305, USA*

ABSTRACT

The feasibility of VLF wave injection using space-borne transmitters is discussed and the radiating antenna characteristics are reported.

INTRODUCTION

In recent years, interactions of energetic radiation belt particles and coherent plasma waves in the earth's magnetosphere have been studied by means of ground-based VLF wave-injection experiments [1,2] in which the amplitude, phase and frequency of the injected waves has been under control of the experimenters. The use of space-borne transmitters for similar experiments has been discussed in different contexts over the last decade [3]. Such transmitters would provide important capabilities not achievable from the ground, namely (1) the ability to create larger power densities by injecting waves directly into the plasma with radiating structures of sizes comparable to the VLF wave length in the medium, (2) the ability to excite a full range of wave normal directions in the plasma, and (3) the ability to study spatial effects through the "source-in-motion" feature.

The proposed Space Shuttle/Space Lab system would provide a useful VLF transmitter platform since it can lift the required large payloads into orbit, erect long antennas, supply the electrical power required, and provide real-time control. In this paper we study the power budget of such a VLF transmitter in an attempt to assess the feasibility of the experiment. In this context, the radiative element is the determining factor, and below we summarize the result of our calculations of the antenna terminal impedance and radiation efficiency for a prototype antenna configuration and parameters. Further details of these results are reported in another paper [4].

ELECTRIC DIPOLE ANTENNA CHARACTERISTICS

A stem-type electric dipole antenna immersed in a magnetoplasma is depicted in Figure 1a. The equivalent circuit for the antenna terminal impedance and the coordinate system are shown in Figure 1b and 1c, respectively. The components of this equivalent circuit are discussed below.

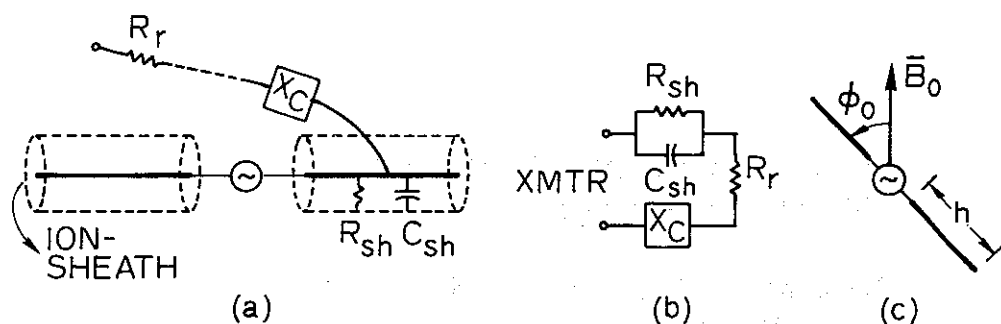


Fig. 1 (a) Electric dipole antenna and the surrounding ion-sheath. (b) Equivalent circuit representation for the terminal impedance. (c) Coordinate system.

The equivalent circuit. The conducting antenna creates an ion-sheath in its immediate vicinity due to the difference between the electron and ion thermal velocities. For small amplitude and low frequency voltages the sheath thickness is sinusoidally modulated at the excitation frequency f , giving rise to a dynamic sheath capacitance C_{sh} and a dynamic sheath resistance R_{sh} . In order to calculate C_{sh} and R_{sh} for parameters suitable to the experiment we have used a formulation [5] which assumes a uniform ion-sheath with a sharp boundary and neglects the effect of the static magnetic field. The results are given in Figure 2.

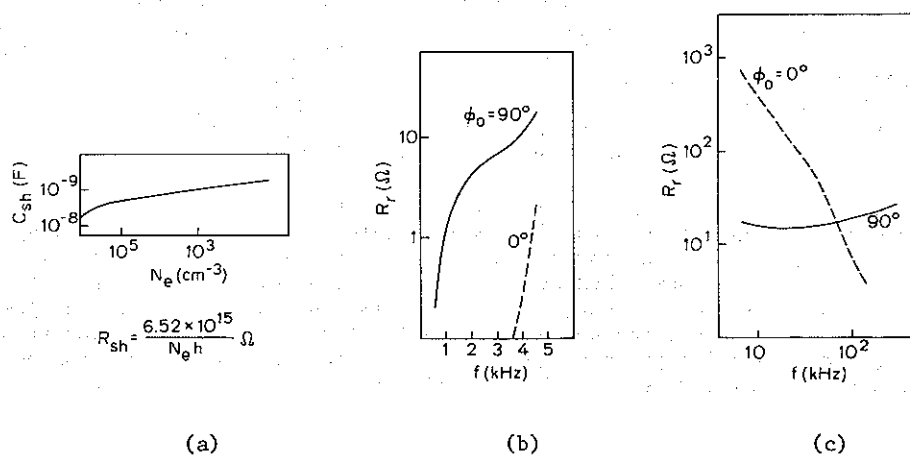


Fig. 2 Typical computed values of the equivalent circuit parameters. (a) The sheath impedance C_{sh} and R_{sh} computed for an ambient electron temperature of 2500°K, a predominantly oxygen plasma, and an antenna velocity of 7 km/sec. (b) The radiation resistance R_r for $N_e = 10^5 \text{ cm}^{-3}$, $h = 150 \text{ m}$ and for $f < f_{LHR}$ for perpendicular ($\phi_0 = 90^\circ$) and parallel ($\phi_0 = 0^\circ$) orientation. (c) R_r for $f > f_{LHR}$.

The cold plasma impedance $Z_C = R_C + jX_C$ accounts for the fields that penetrate into the plasma. Using the formulation of Wang [6] to determine Z_C , it can be shown that for $f \neq f_{LHR}$ (lower hybrid resonance frequency) the input impedance of the dipole antenna is dominated by the r-f sheath impedance and the real part of the cold plasma impedance, namely the radiation resistance $R_r = R_C$. We have calculated R_r for the case of a cold multicomponent magnetoplasma with a static magnetic field $B_0 \approx 0.2$ Gauss, electron density $N_e \approx 10^4 - 10^6$ el/cc, and plasma composition of 90% O^+ and 10% H^+ , representing typical ionospheric conditions at ~ 350 km altitude. In this anisotropic medium, R_r is a complicated function of frequency and antenna orientation ϕ_0 , as well as the plasma composition and N_e . The results are given in Figure 2b for $f < f_{LHR}$ and in Figure 2c for $f > f_{LHR}$. The behavior of the antenna changes markedly at $f \approx f_{LHR}$ [6].

Note that we have assumed a cold plasma in our calculations. In case of a warm plasma, thermal modes as well as the whistler-mode waves will be excited. However, even in this case it has been shown that $>80\%$ of the power represented by R_r can be coupled into the whistler mode [6].

Antenna terminal impedance and radiation efficiency. With the equivalent circuit model of Figure 1 we can calculate the real and imaginary parts of the antenna terminal impedance, namely Z_R , Z_X , and the radiation efficiency, $\eta \equiv R_r/Z_R$, for various ranges of parameters. In all these calculations, we have used a static magnetic field $B_0 \approx .2$ Gauss and a plasma composition of 90% O^+ and 10% H^+ at 350 km altitude. The computed values of Z_R , Z_X for all the cases considered in this paper lie in the region designated by the dashed lines in Figure 3.

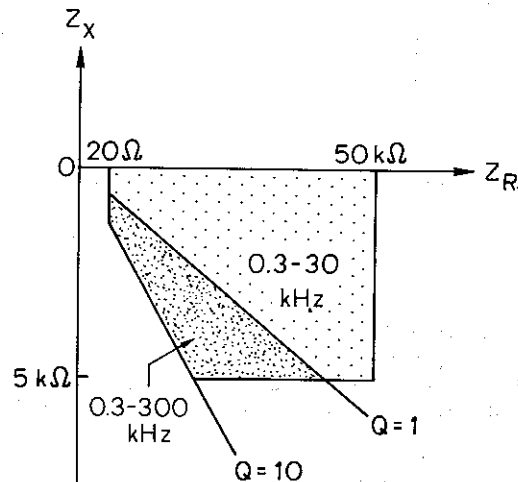


Fig. 3 The impedance range of the electric dipole antenna for the parameter values considered in this paper.

The variations of the radiation efficiency η with N_e , dipole half-length h and antenna orientation ϕ_0 are shown in Figure 4.

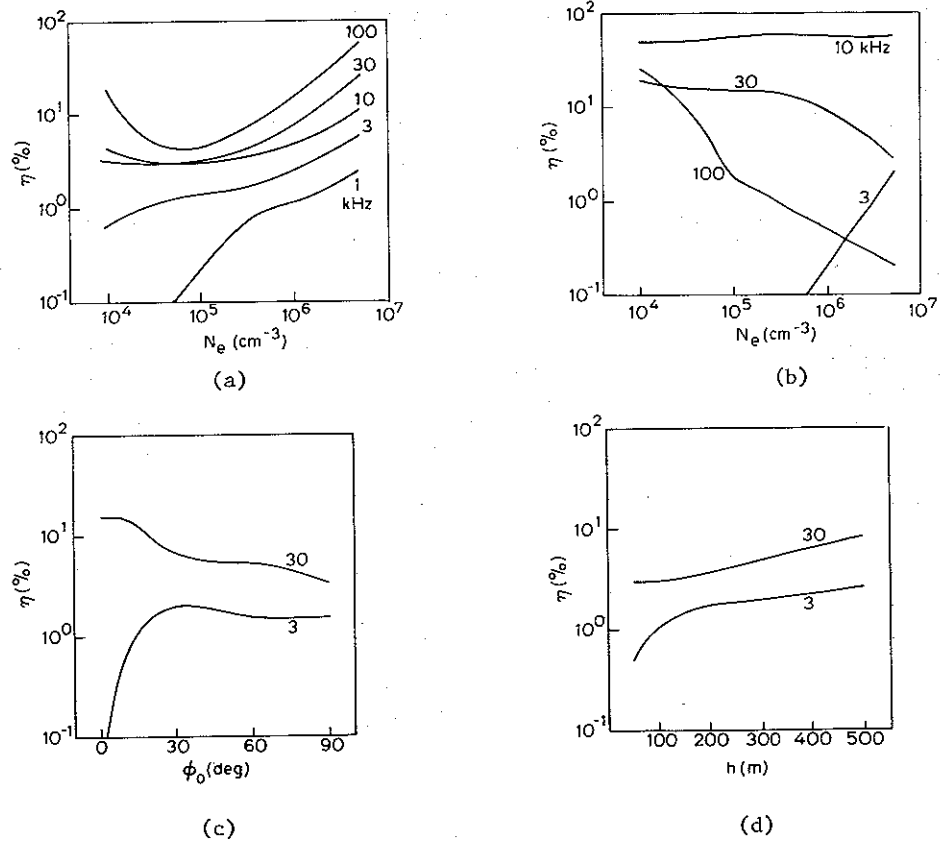


Fig. 4 (a) The antenna radiation efficiency η vs N_e for different frequencies, for $\phi_0 = 90^\circ$, $h = 150$ m. (b) Same for $\phi_0 = 0^\circ$. (c) η vs antenna orientation ϕ_0 , for $N_e = 10^5 \text{ cm}^{-3}$, $h = 150$ m and $f = 3$ ($< f_{\text{LHR}}$) and 30 kHz ($> f_{\text{LHR}}$). (d) η vs dipole half-length h , for $N_e = 10^5 \text{ cm}^{-3}$, $\phi_0 = 90^\circ$ and $f = 3$ and 30 kHz.

DISCUSSION AND CONCLUSIONS

For any given input power level into the antenna terminals the radiation efficiencies reported above determine the total power radiated into the whistler mode. In the anisotropic plasma environment the radiation pattern of the dipole antenna provides an additional effective gain of up to 40 dB in launching waves with certain ray directions (e.g., along \vec{B}_0 for $f > f_{\text{LHR}}$) [7]. In addition, once the waves are launched, they will propagate away from the antenna and can be focused in the vicinity of magnetospheric density gradients [8].

According to Figure 3 the antenna behaves as a low Q (< 10) element for most of the impedance range considered. Thus the tuning of the antenna is not a critical factor

and the radiated power is determined mainly by the efficiency η .

On the basis of these results we conclude that a 1-10 kW transmitter placed on the Space Shuttle/Space Lab system and coupled into a stem-type electric dipole of ~150 m half-length can inject from one watt to up to a few kilowatts of wave power into the whistler mode. Recent results of ground-based VLF wave-injection experiments show that such power levels would be more than enough for initiating nonlinear wave growth and amplification and emission triggering in the magnetosphere. Theoretical calculations based on test particle computer simulation of the wave-particle interaction indicate that the generated waves would interact strongly with the radiation belt particles and precipitate significant energy fluxes into the ionosphere [9]. We can thus conclude that a Shuttle-based VLF transmitter experiment is not only feasible but will also greatly increase our understanding and control of the wave-particle interaction mechanism in the magnetosphere.

ACKNOWLEDGMENTS

We wish to acknowledge the many valuable discussions we have held with our colleagues in the Radioscience Laboratory during the course of this work. The final manuscript was prepared by K. Dean. This research was supported by the National Aeronautics and Space Administration under contract NGL-05-020-008.

REFERENCES

1. R. A. Helliwell and J. P. Katsufakis, J. Geophys. Res. **79**, 2511 (1974).
2. H. C. Koons, M. H. Dazey, R. L. Dowden, and L. E. S. Amon, J. Geophys. Res. **81**, 5536 (1976).
3. Final Report of the Science Definition Panel for AMPS Space Lab Payload, Universities Space Research Association, P.O. Box 1892, Houston, Texas 77001, 1976.
4. U. S. Inan, T. F. Bell, and R. A. Helliwell, J. Geophys. Res. (in press) (1980).
5. R. F. Mlodnosky and O. K. Garriott, in: Proc. Intern. Conf. on the Ionosphere, The Institute of Physics and the Physical Society, 1963, p. 484.
6. T. N. C. Wang, Tech. Rep. 3414-1, Radioscience Lab., Stanford Electron. Lab., Stanford University, Stanford, Calif. 94305, 1970.
7. T. N. C. Wang and T. F. Bell, J. Geophys. Res. **77**, 1174 (1972).
8. U. S. Inan and T. F. Bell, J. Geophys. Res. **82**, 2819 (1977).
9. U. S. Inan, T. F. Bell, and R. A. Helliwell, J. Geophys. Res. **83**, 3235 (1978).

1. The first part of the document discusses the importance of maintaining accurate records of all transactions and activities. It emphasizes that this is essential for ensuring transparency and accountability in the organization's operations.

2. The second part of the document outlines the various methods and tools used to collect and analyze data. It highlights the need for consistent data collection procedures and the use of advanced analytical techniques to derive meaningful insights from the data.

3. The third part of the document focuses on the implementation of data-driven decision-making processes. It discusses how the collected data is used to identify trends, assess risks, and make strategic decisions that align with the organization's goals.

4. The fourth part of the document addresses the challenges and limitations of data analysis. It notes that while data provides valuable insights, it is not infallible and must be interpreted with care, taking into account potential biases and uncertainties.

5. The fifth part of the document discusses the future of data analysis and the role of emerging technologies. It mentions that advancements in artificial intelligence and machine learning are expected to significantly enhance the capabilities of data analysis in the coming years.

6. The sixth part of the document provides a summary of the key findings and conclusions. It reiterates the importance of a robust data management system and the continuous monitoring and evaluation of data analysis processes.

7. The seventh part of the document offers recommendations for improving data analysis practices. It suggests that organizations should invest in training, technology, and infrastructure to ensure they are fully equipped to handle the growing volume and complexity of data.

8. The eighth part of the document discusses the ethical implications of data analysis. It emphasizes the need for organizations to adhere to strict ethical guidelines and ensure that data is used responsibly and transparently.

9. The ninth part of the document provides a final overview of the document's content and its relevance to the organization. It concludes by stating that the insights gained from this analysis will be used to inform future strategic planning and operational improvements.

10. The tenth part of the document is a concluding statement that expresses the author's confidence in the findings and their potential impact on the organization's success. It also expresses a commitment to ongoing research and innovation in the field of data analysis.